NEOPLASIA
www.neoplasia.com

Volume 23 Number 12 December 2021 pp. 1289–1299

Nucleostemin upregulation and STAT3 activation as early events in oral epithelial dysplasia progression to squamous cell carcinoma

Madeleine Crawford[a,1]; Xiaoqin Liu[a,1]; Yi-Shing L Cheng[b,*]; Robert YL Tsai[a,c,**]

[a] Institute of Biosciences and Technology, Texas A&M Health Science Center, 2121 W Holcombe Blvd, Rm 517, Houston, Texas 77030, USA
[b] Department of Diagnostic Sciences, Texas A&M University College of Dentistry, 3302 Gaston Ave, Dallas, Texas 75246, USA
[c] Department of Translational Medical Sciences, Texas A&M Health Science Center, Houston, Texas 77030, USA

Abstract

Most low-grade oral epithelial dysplasia remains static or regress, but a significant minority of them (4–11%) advances to oral squamous cell carcinoma (OSCC) within a few years. To monitor the progression of epithelial dysplasia for early cancer detection, we investigated the expression profiles of nucleostemin (NS) and phospho-STAT3 (p-STAT3) in rodent and human samples of dysplasia and OSCCs. In a 4NQO-induced rat oral carcinogenesis model, the number and distribution of NS and p-STAT3-positive cells increased in hyperplastic, dysplastic, and neoplastic lesions compared to normal epithelium. In human samples, the NS signal significantly increased in high-grade dysplasia and poorly differentiated OSCC, whereas p-STAT3 was more ubiquitously expressed than NS and showed increased intensity in high-grade dysplasia and both well and poorly differentiated OSCC. Analyses of human dysplastic samples with longitudinally followed outcomes revealed that cells with prominent nucleolar NS signals were more abundant in low-grade dysplasia that advanced to OSCC in 2 or 3 years than those remaining static for 7–14 years. These results suggest that NS upregulation and STAT3 activation are early events in the progression of low-grade dysplasia to OSCC.

Neoplasia (2021) 23, 1289–1299

Keywords: Cancer prevention, Leukoplakia, Oral epithelial dysplasia, Oral premalignant lesion, Prognosis prediction, Risk assessment

Novelty and Impact: Tracking the progression of oral dysplasia to cancer or predicting its risk in becoming cancer are clinically important for achieving early detection of cancer for early diagnosis/treatment or evidence-based management of precancerous lesions for cancer prevention, respectively. Nucleostemin and phospho-STAT3 show increased signal intensity during early oral carcinogenesis. Furthermore, dysplasia with rapid progression to cancer show more nucleolar signals of nucleostemin than those remaining static, indicating its mechanistic role and clinical value in driving and/or tracking dysplasia-to-OSCC progression.

Introduction

Oral cancer is the 8th and 15th most common cancer for men and women in the US, respectively [1]. Despite recent advances in diagnosis and therapies, its five-year survival rate remains at 66% (American Cancer Society, 2021). Oral squamous cell carcinoma (OSCC) is the most common type of oral cancer (>90%). OSCCs normally develop from clinically visible oral premalignant lesions (OPLs), also known as leukoplakia or erythroplakia. Histologically, OPLs include hyperkeratosis, low-grade (mild or moderate) dysplasia, or high-grade (severe dysplasia). Probability for low-grade and high-grade dysplasia to become cancer are 4–11% and 35%, respectively [2]. Although the majority of low-grade dysplasia remain static or regress spontaneously, the 4–11% that don't still account for a significant number of patients, considering the size of the population affected by this disease. As a result, there is a critical need to find new markers for detecting early-stage cancers or predicting the risk of OPLs in developing OSCCs.

The best strategy to treat OSCCs is to eliminate dysplasia before they become cancerous. However, the decision to remove low-grade dysplasia is not without concerns. Surgery and laser ablation can cause severe local

Abbreviations: 4-nitroquinoline-1-oxide, (4NQO); head and neck squamous cell carcinoma, (HNSCC); immunohistochemistry, (IHC); nucleostemin, (NS); oral premalignant lesion, (OPL); oral squamous cell carcinoma, (OSCC); phospho-STAT3, (p-STAT3); Short-Tagged Sequence, (STS); Sprague-Dawley, (SD).

* Corresponding author at: Department of Diagnostic Sciences, Texas A&M University College of Dentistry, 3302 Gaston Ave, Rm 222, Dallas, Texas 75246, USA.
** Corresponding author at: Institute of Biosciences and Technology, Texas A&M Health Science Center, 2121 W Holcombe Blvd, Rm 517, Houston, Texas 77030, USA.
E-mail addresses: ycheng@tamu.edu (Y.-S.L. Cheng), robtsai@tamu.edu (R.Y. Tsai).
[1] These authors contribute equally to this work.

Received 8 September 2021; received in revised form 27 October 2021; accepted 1 November 2021

https://doi.org/10.1016/j.neo.2021.11.001

discomfort and side effects, especially for lesions that are large in size, diffuse, multifocal, or recurrent. They are also limited by cost and availability. Medications may introduce systemic toxicity. Therefore, it is difficult to justify the use of invasive or systemic therapies to treat low-grade dysplasia, unless their risk of becoming OSCC can be further stratified. To date, there are many published studies looking for prognostic immunohistochemistry (IHC) markers for OSCC [3]. Among them, all but two used post-diagnostic samples with retrospective designs. Of the two prospective studies, only one focused on the malignant transformation risk of dysplasia, the results of which showed that dysplasia with higher positive percentages of aldehyde dehydrogenase 1-A1 (ALDH1A1) and prominin 1 (PROM1) may be more likely to develop OSCC [4]. ALDH1 and PROM1 have been implicated in maintaining the self-renewal of cancer stem cells.

Key information on OPL-to-OSCC progression may be gained by studying the expression profiles of other stem cell self-renewal factors [5]. *Nucleostemin (NS)* was first discovered in neural and embryonic stem cells [6–8] and later found to be expressed at high levels in many other stem cell types as well as regenerating tissues [6–10]. It belongs to a family of three GTP-binding nucleolar proteins [9,11–13]. In most cancer types, NS is linked to high-grade malignancy and poor prognosis [6,14–17]. One early study reported that head and neck squamous cell carcinoma (HNSCC) is associated with a significant enlargement of NS-positive nucleoli [18]. One group initially reported wide NS expression in normal and neoplastic oral epithelial tissues [19] but later showed that NS overexpression contributed to the malignancy and poor prognosis of OSCC via *STAT3* activation [20]. NS overexpression was also associated with phosphorylated STAT3 (p-STAT3) upregulation in glioblastoma multiforme [21] and hepatocellular carcinoma [22]. *STAT3* belongs to a family of transcription factors that regulates multiple pathways involved in tumorigenesis and is activated via tyrosine phosphorylation [23]. p-STAT3 has previously been investigated as a potential prognostic biomarker in predicting poor survival outcome for several cancers, including OSCC [24,25]. Its expression in pre-malignant lesions remains to be determined.

To explore the potential roles of NS and STAT3 in the progression of OPLs, we analyzed their expression profiles in archival human biopsy samples of dysplasia and OSCC, including a group of low-grade dysplasia samples with longitudinal follow-up biopsies showing clinical outcome, and 4-nitroquinoline-1-oxide (4NQO)-treated rats. 4NQO produces oxidative stress that leads to guanosine replacement by adenosine, closely resembling genomic insults caused by tobacco-related carcinogens. 4NQO-induced oral lesions also underwent the same multi-step progression from OPL to OSCC and bear a high histological and molecular resemblance to tobacco-induced human OSCC [26–29]. Using the 4NQO-treated rat model and human samples, we showed that cellular intensity and distribution of NS and/or p-STAT3 signals could track the early progression of low-grade dysplasia and differentiate between low-grade dysplasia samples that remained static or progressed to OSCC in 2 or 3 years.

Materials and methods

Animal care and 4NQO treatment

Animals were housed by the Program for Animal Resources at the Texas A&M Health Science Center-Houston campus and handled in accordance with the principles described by the *Guide for the Care and Use of Laboratory Animals*, following the procedures approved by the IACUC. Male Sprague–Dawley (SD) rats (3-week-old) were purchased from ENVIGO, housed in a room with a barrier system, and maintained at 23 ± 2 °C, 55 ± 5% relative humidity, and a 12 h light–dark cycle, with free access to diet and drinking water. After 3 weeks of acclimatization, rats were fed with 4-nitroquinoline-1-oxide (4NQO) water for OPL/OSCC induction. 4NQO (N8141, Sigma, Saint Louis, MO) was dissolved in propylene glycol to make a 4 mg/mL stock solution and diluted to 50 μg/mL (50 ppm) in acidified distilled water. 4NQO water was replaced twice a week. Throughout the feeding process, rats were monitored for body weight, food/water intake, and motor activity. Animals showing severe body wight loss or morbidity were euthanized. For the time-course study, eight animals per group were randomly selected and sacrificed to collect whole tongue tissues after 12 weeks (12w), 16w, 20w, and 24w of 4NQO treatment. Serial sections were collected on every 8 sections throughout the whole tongue in a lesion-blind manner for H&E staining and pathology evaluation. On average, 18–27 sections were analyzed for every tongue. For IHC studies, three pathologically confirmed samples from four animals were examined for each lesion type.

Histopathological analysis

Formalin-fixed paraffin-embedded (FFPE) sections of human oral mucosal samples were obtained from de-identified patient archival biopsy samples in the Texas A&M University College of Dentistry. The majority of the samples were incisional biopsies collected from relatively large-sized lesions located mostly on the tongue but occasionally at other oral anatomic sites, such as the buccal mucosa, gingiva, palate, or mouth floor. This study was reviewed by the institutional IRB committee and determined as Not Human Research by DHHS and FDA regulations. Normal epithelial tissues were obtained from samples diagnosed with fibroma. Rodent tissue and biopsy samples (four animals per lesion types) were collected from 4NQO-treated rats, fixed in 10% buffered formalin, and embedded in paraffin blocks. Sections (4 μm thickness) were processed for H&E and IHC staining, and examined by a board-certified oral pathologist in a blinded manner. Hyperplasia is defined as thickening (increased cell number) of the spinous cell layer of the surface epithelium without cellular atypia. Low-grade dysplasia is defined by the presence of atypical cellular and/or architectural changes that occupy the lower half of the epithelial thickness, including hyperchromatism, pleomorphism, increased nuclear-to-cytoplasmic ratio, rounding of the rete ridges, nuclear crowding, multi-nucleation, and dyskeratosis. High-grade dysplasia is defined by the presence of atypical cellular and/or architectural changes that occupy more than the lower half of the epithelial thickness but are still confined within the epithelium. OSCC is defined as a malignancy arising in the surface squamous epithelium that has broken through the basement membrane and invaded the underlying tissue, such as the skeletal muscle.

Immunohistochemistry analysis

For IHC studies, sections were dewaxed and rehydrated, treated with 0.3% H_2O_2, and antigen-retrieved in boiling 10 mM Tris solution (with 1 mM EDTA pH9). Immunohistochemistry was performed by incubation with primary antibodies, followed by biotin-labeled secondary antibodies, avidin-conjugated HRP, and DAB color reaction. Primary antibodies used in this study include anti-rat NS (Ab2438, Tsai Lab), anti-human NS (Ab138, Tsai Lab), p-STAT3 (Tyr705, Cell Signaling, 9145TS, Danvers, MA), and Ki67 (Spring Bioscience, M3064, Pleasanton, CA). The specificity of Ab2438 and Ab138 was previously validated [7,13,30]. For quantitative analysis, three images were taken for each sample using a Zeiss 20 × Plan-APO objective. For each image, the epithelium was divided into a lower and an upper half. Areas of these two parts of the epithelium were measured using the NIH Image J v1.53 software calibrated based on a micrometer, where 7.3836 pixels equaled 1.0 μm. Cells with positive nucleolar NS signals were defined by their prominent nucleolar staining with little-to-no diffuse nuclear staining. Cells with diffuse nuclear NS signals were defined by diffuse nuclear signal staining without prominent nucleolar staining. Positive signals were manually counted in a blinded manner and then compared between groups using a nonparametric two-tailed TTEST analysis with a 95% confidence interval, where a significant difference was defined by a p value ≤ 0.05.

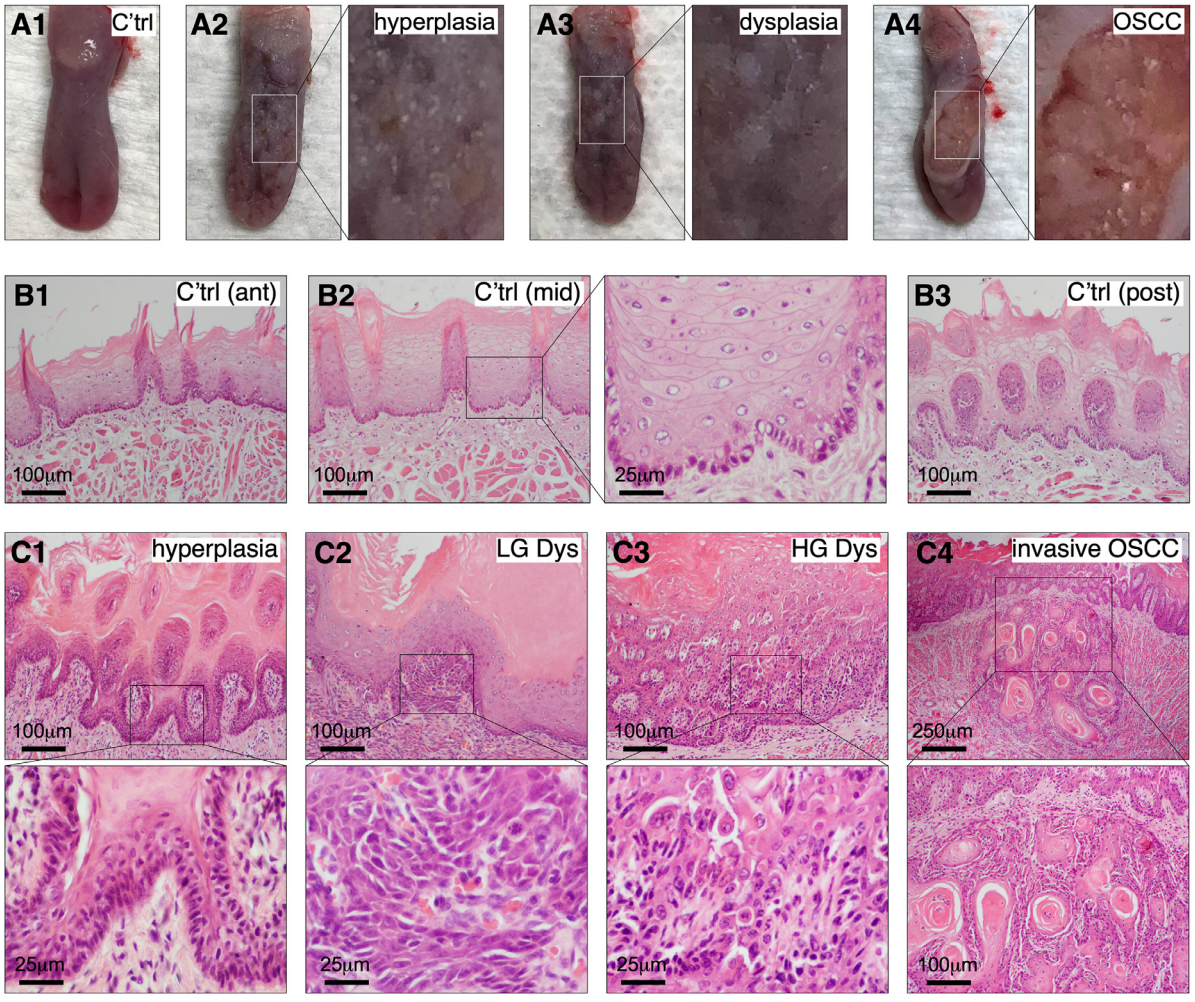

Fig. 1. 4NQO-treated Sprague-Dawley (SD) rats display a continuous spectrum of oral carcinogenic lesions. Dorsal views of rat tongues with normal surface (A1, C'trl), hyperplasia (A2), dysplasia (A3), and ulcerative OSCC (A4). H&E morphology of normal oral epithelium in the anterior (B1), mid (B2), and posterior dorsal tongue (B3). H&E morphology of 4NQO-treated tongues with hyperplasia (C1), low-grade dysplasia (C2), high-grade dysplasia (C3), and invasive OSCC (C4). The right panel in (B2) and bottom panels in (C) show enlarged images indicated by insets.

Real-time PCR assays

Oral tissues were collected from mucosal lesions located on the dorsal surface of the tongue. All lesions were verified by H&E staining of their pathology. Total DNAs were purified by proteinase K (100 μg/mL) digestion in STEN buffer (1% SDS, 0.1 M NaCl, 0.01 M EDTA pH 8.0, 0.05 M Tris pH 7.5), followed by phenol-chloroform extraction. Q-PCR reactions were carried out using the MyiQ single-color real-time PCR detection system and supermix SYBR green reagent (Bio-Rad, Hercules, CA). The $\Delta C(t)$ values were determined by comparing the target message to the reference message (POLR2A). The $\Delta\Delta C(t)$ values were measured from 6 biological replicates, each with two technical repeats. Tm was set at 60 °C for all reactions. Primer sequences are listed in Fig. S1.

Results

4NQO-treated rats display a continuous spectrum of oral carcinogenesis

To determine the expression profiles of NS and p-STAT3 in a preclinical model of oral carcinogenesis, we used 4NQO to induce OPLs and OSCCs in male Sprague Dawley (SD) rats. Most 4NQO-treated SD rats began to show patchy white lesions on their dorsal tongue surface after 10–12 weeks of treatment (Figs. 1A1–3). After 16 weeks of treatment, a few animals developed more severe ulcerative lesions (Fig. 1A4). H&E staining showed that 4NQO-treated SD rats developed a continuous spectrum of oral preneoplastic and neoplastic lesions, ranging from hyperplasia, low-grade dysplasia, high-grade dysplasia, carcinoma *in situ* (CIS), to invasive OSCC, bearing a high histological resemblance to human OPLs and OSCCs. Compared to non-4NQO-treated rats (Fig. 1B), those treated with 4NQO for 12 or 16 weeks showed a wide range of lesions, including hyperkeratosis, hyperplasia (Fig. 1C1), low-grade dysplasia (Fig. 1C2), high-grade dysplasia (Fig. 1C3), CIS, and invasive carcinoma (Fig. 1C4).

Unlike human lesions, all OSCCs observed in 4NQO-treated rats were well differentiated. Notably, rats surviving 20–24 weeks of 4NQO treatment demonstrated less severe lesions compared to those sacrificed after 12–16 weeks of treatment. Based on the most severe lesion found on individual tongues, rats treated with 12 or 16 weeks of 4NQO displayed similar frequencies of lesion types from hyperplasia to SCC, whereas rats surviving a 20–24-week 4NQO treatment showed mostly dysplastic lesions and very few had invasive carcinomas (1 in 16). Specifically, rats examined at 12–16 weeks of 4NQO treatment demonstrated three cases of hyperkeratosis, two hyperplasia, six low-grade dysplastic lesions, one high-grade dysplastic lesion, and four rats with SCC. Contrarily, rats surviving 20–24 weeks of treatment presented with no hyperkeratosis, one occurrence of hyperplasia,

eight low-grade dysplastic lesions, five high-grade dysplastic lesions, and only one case of CIS and one case of OSCC (Table S1). These findings indicate that a 12–16-week treatment of 4NQO at 50 ppm is sufficient to induce a spectrum of oral carcinogenic lesions and suggests that individual outbred SD rats may show differential sensitivities to 4NQO-induced carcinogenesis. Factors that determine the early (sensitive) vs. late (resistant) responders remain unknown. Of note, rats receiving 4NQO-containing drinking water also developed malignancy throughout their alimentary tract, which might require early euthanasia due to animal welfare consideration, thereby limiting further development of OSCC in this model.

Expression profiles of Ki67, NS, and p-Stat3 in 4NQO-induced oral lesions

The expression profiles of Ki67, NS, and p-STAT3 in 4NQO-induced OPL and OSCC lesions were determined by immunohistochemistry (IHC) ($n = 4$). Anti-Ki67 staining showed that Ki67-positive proliferative cells were present in subsets of basal cells in the normal and hyperplastic oral epithelium. The hyperplastic epithelium showed stronger signal intensity and more positive cells than the normal epithelium. In dysplasia and OSCC, Ki67-positive cells showed stronger signal intensity than the normal epithelium, and were found beyond the basal layer, including the lower-half of the epithelium in low-grade dysplasia, the whole epithelium in high-grade dysplasia, and the submucosal layer in OSCCs (Fig. 2A). NS signals, which were relatively absent in the normal epithelium, increased significantly in the hyperplastic, dysplastic (low-grade and high-grade), and carcinomatous lesions. Of the four different types of lesions, differences resided mainly in the distribution of NS-positive cells but not in the signal intensity of individual cells *per se*, with NS-positive cells present in the basal/suprabasal layers for hyperplasia, in the lower-half of the epithelium for low-grade dysplasia, in the whole epithelium for high-grade dysplasia, and in the tumor islands in lamina propria for OSCC (Fig. 2B). Similar to NS, the p-STAT3 signal was absent in the normal epithelium and increased in the hyperplastic, dysplastic, and carcinomatous lesions. Hyperplastic, dysplastic, and carcinomatous lesions differed more in the distribution of p-STAT3-positive cells than in the signal intensity of individual cells (Fig. 2C). Unlike NS, p-STAT3 signals in the hyperplastic lesion were found in subsets of basal cells, whereas the NS signal was also found in some suprabasal cells. Together, our results showed that the cellular intensity of NS and p-STAT3 signals increased most significantly during the transition from normal to hyperplastic epithelium, and the number and distribution of positive cells increased as lesions progress from hyperplastic, low-grade dysplastic, high-grade dysplastic to carcinomatous lesions. As the Ki67 signal was present in a subset of basal cells in the normal epithelium with lower intensity, these findings suggest that NS and p-STAT3 are expressed in hyperactive mitotic cells and these markers may indicate early dysplastic changes.

Changes of short-tagged sequence (STS) genetic markers occur late in 4NQO-induced lesions

Next, STS-based markers were investigated to determine if they can better detect and differentiate oral dysplastic and/or early carcinogenic lesions compared to NS or p-STAT3 IHC markers. STS markers are short stretches of DNA that are detectable by PCR and uniquely represent single sites in the genome. Based on the results of a previous study that identified genetic loci linked to the differential susceptibilities of Dark-Agouti (DA) and Wistar/Furth (WF) rats to 4NQO-induced tongue cancers [31], seventeen STS markers were selected, located on rat chromosome 1 (RNO1) ($n = 10$), RNO4 ($n = 2$), RNO5 ($n = 3$), and RNO6 ($n = 2$) (Fig. 3A). Levels of these STS markers in normal and 4NQO-induced hyperplastic, dysplastic, or carcinomatous oral lesions in SD rats were measured by qPCR assays and their copy number gain or loss was compared to the RNA Polymerase II subunit A (Polr2a) locus. Sites showing $\geq$ 50% copy number increase (or decrease) in lesions compared to normal tissues were considered gain (or loss) of heterozygosity. Twelve STS markers displayed gain of heterozygosity with p values ≤ 0.05 in dysplastic and/or carcinomatous lesions; none showed loss of heterozygosity (Fig. 3B). Eight showed $\geq$ 50% increase in OSCC only (D1Mgh21, D1Wox22, D1Mit5, D1Mgh10, D1Rat213, D4Mgh18, D5Mit111, and D6Rat55), two in dysplasia only (D1Rat27, D1Rat320), one in both dysplasia and OSCC (D1Wox36), and one in all hyperplasia, dysplasia, and OSCC (D6Rat45). Of those changes, only D1Mgh21 showed a 2.5 × increase in OSCC compared to other types of lesions, and D6Rat45 showed a 2.5 × increase in OSCC and a ~2 × increase in hyperplastic and dysplastic lesions compared to the normal epithelium. As a reference, the genetic locus of NS showed a < 1.5-fold change. These results indicate that unlike NS and p-STAT3 expression, genetic gain (or loss) occurs more commonly in late-stage oral carcinogenic lesions.

Expression profiles of NS and p-STAT3 in human cross-sectional samples of dysplasia and OSCC

Expression patterns of NS and p-STAT3 in human tissues of normal epithelium (fibroma), low- and high-grade oral dysplasia, and well and poorly differentiated OSCCs were determined by immunohistochemistry. Three samples for each lesion type were analyzed (Fig. 4A). In normal oral epithelium, weak NS signals were found mainly in the basal and parabasal cells and a few cells scattered in the lower spinous cell layer (Fig. 4B). Most NS signals in the basal cell layer of normal epithelium were diffuse in the nucleus. Only a few in the parabasal cell layer showed 2–4 discrete low-level nucleolar signals. In low-grade dysplastic lesions, the number of NS+ cells increased in the lower-half of the oral epithelium, corresponding with the appearance of dysplastic cells with basoloid morphology (increased nuclear to cytoplasmic ratio). More cells expressed ≥5 positive-stained dots within the nuclei, but the signal intensity within individual cells remained relatively low. In high-grade dysplastic lesions, NS was expressed in almost all dysplastic cells in the spinous cell layer distributed throughout the whole thickness of the epithelium, and the nucleolar intensity of NS signals showed a significant increase in some cells. In well differentiated SCC, NS was generally expressed at a much lower level and found only in a few tumor cells located at the periphery of tumor islands. NS signals within those cells were less in number and not as prominent. Notably, NS was expressed at the highest level in poorly differentiated SCC, present in almost all tumor cells, and NS-positive nucleolar signals were prominent, demonstrating various shapes and sizes. The distribution and intensity of the nucleolar NS positive signals increased from low-grade dysplastic lesions to poorly differentied OSCC, in comparison to the weak diffuse signal present in the normal epithelium. For p-STAT3 staining, low-to-moderate intensity signals were found in the nuclei of most cells in the basal, suprabasal and spinous cell layers in the normal epithelium (Fig. 4C). In low-grade and high-grade dysplasia as well as OSCC, p-STAT3 signal intensity increased in individual cells, with OSCC lesions showing some cells with strong p-STAT3 signals. Together, these findings suggest that the expression pattern of NS (*i.e.*, signal intensity and distribution) may be useful for differentiating normal, early, and late dysplastic lesions, as well as differentiating well vs. poorly differentiated OSCCs, whereas the STAT3 signal is more uniformly activated in human dysplastic and OSCC lesions.

Expression analysis of NS and p-STAT3 in progressive vs. static human dysplasia samples

To determine whether NS (or p-STAT3) behaves differently in human low-grade dysplasia with different outcomes of progression, we reviewed formalin-fixed paraffin-embedded archival samples of oral dysplasia and

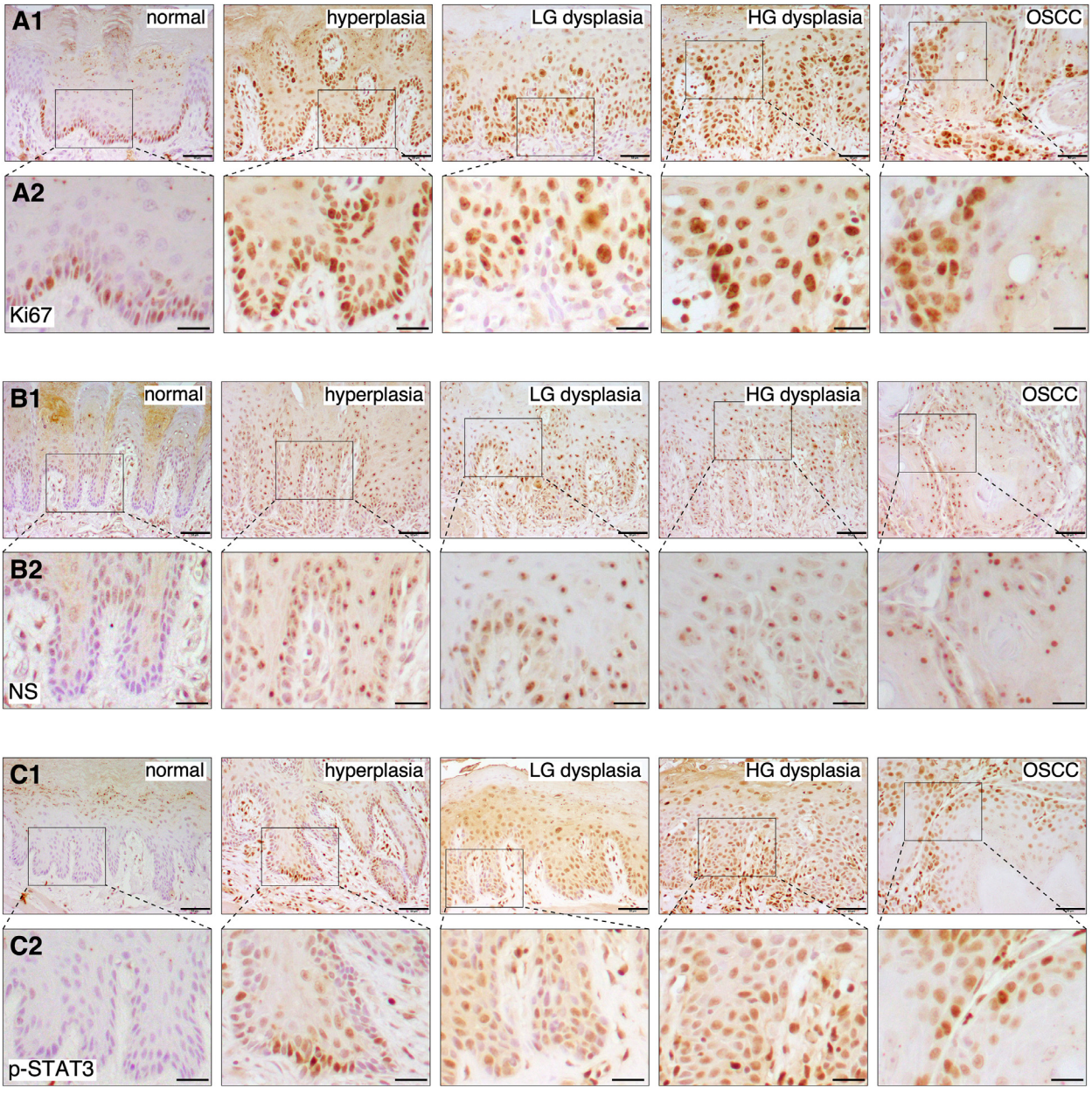

Fig. 2. Expression profiles of nucleostemin (NS) and phospho-STAT3 (p-STAT3) at different stages of OSCC development in 4NQO-treated rats. Immunohistochemistry of Ki67 (A), NS (B), and p-STAT3 (C) in normal, hyperplastic, low-grade (LG) dysplastic, high-grade (HG) dysplastic, and carcinomatous oral lesions (OSCC) collected from control or 4NQO-treated rats (4 samples per lesion types). All IHC images, including normal tissues, were counterstained with hematoxylin (blue/purple) on top of DAB signals (brown). Scale bars show 50 μm for (A1, B1, C1) and 20 μm for (A2, B2, C2). (For interpretation of the references to color in this figure legend, the reader is referred to the web version of this article)

OSCC from patients with multiple biopsies and longitudinal clinical follow-up information in the Department of Diagnostic Sciences, Texas A&M College of Dentistry. Eight patients with tobacco-related dysplasia were identified that showed two distinct outcomes of progression. Four patients in the progressive group showed low-grade oral dysplasia in their first biopsy and developed OSCC at the same lesion sites within 2 or 3 years. Four patients in the static group showed low-grade oral dysplasia in their first biopsy and remained the same for 7–14 years, confirmed by the follow-up biopsy (Figs. 5A, B).

NS-positive signals were observed in both the lower-half and the upper-half of the oral epithelium. Two NS signal patterns were found. A nucleolar pattern describes cells that presented a prominent nucleolar signal with little-to-no diffuse nuclear staining. A diffuse nuclear (hereafter called nuclear) pattern denotes cells with a diffuse nuclear signal without prominent nucleolar staining. In progressive dysplasia, the number of cells with nucleolar NS signals was significantly higher in the lower epithelium than in the upper epithelium ($p = 0.03$), which is in line with increased proliferative activity in the basal layer (Fig. 6A1 and C1). In static dysplasia, the number of cells with nuclear NS signals appeared to be more in the lower epithelium than in the upper epithelium but the difference was not yet statistically significant ($p = 0.09$) (Fig. 6A2 and C2). Most importantly, the number of cells with nucleolar NS signals was higher in progressive dysplasia than in static dysplasia, either in the lower-half of the epithelium ($p = 0.02$) or throughout the whole epithelium ($p = 0.05$) (Fig. 6A, C1). The number of cells with

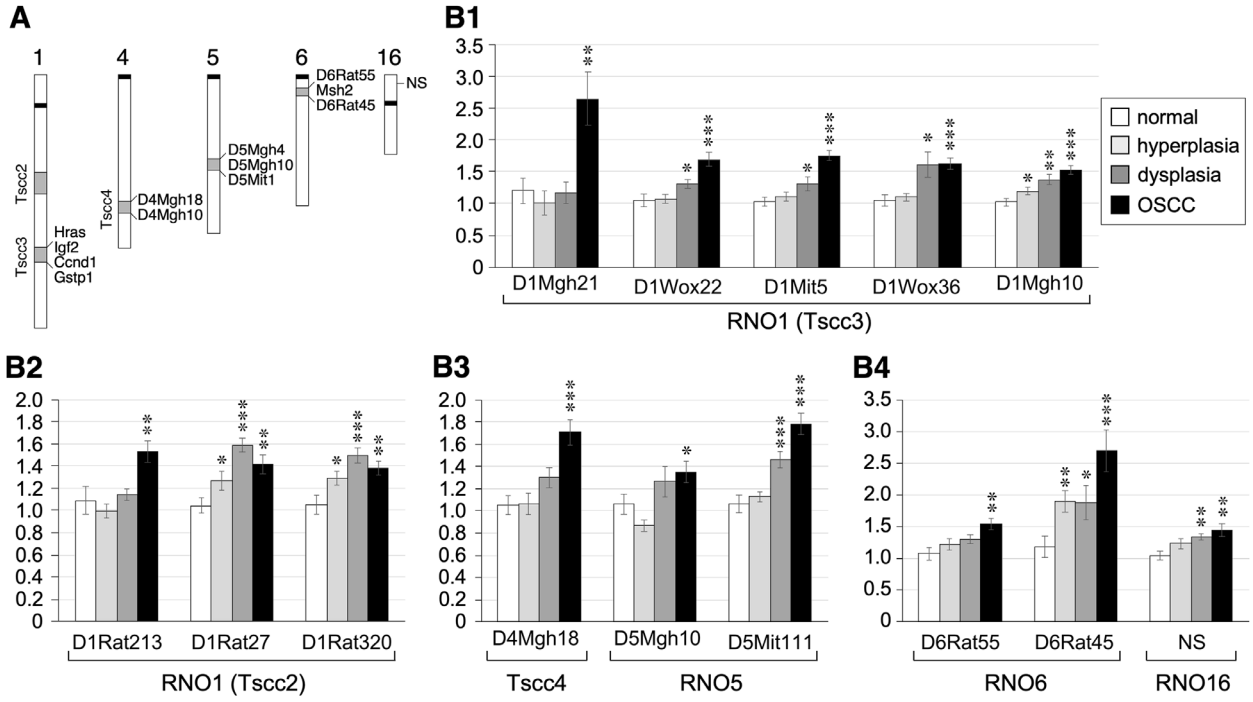

Fig. 3. Quantification of Short-Tagged Sequence (STS) markers in 4NQO-induced oral lesions. A schematic diagram of the genomic loci of seventeen STS markers and NS. Some neighboring genes in the Tscc3 and RNO6 regions are listed. (B) Quantitative PCR analyses of selected STS markers showing changes in 4NQO-induced lesions compared to normal epithelium ($n = 12$). Bar graphs show means (± s.e.m). Asterisks indicate p values <0.05 (*), <0.01 (**), or <0.001 (***).

nuclear NS signals appeared to be higher in static dysplasia than in progressive dysplasia, but the difference was not yet statistically significant ($p = 0.10$) (Fig. 6A, C2). p-STAT3 staining showed a diffuse nuclear pattern with a moderate-to-high intensity. The average number of p-STAT3+ cells appeared to be higher in the lower-half than in the upper-half of the epithelium, but the difference was not statistically significant due to large variability for both progressive and static dysplasia (Fig. 6B, C3). For the same reason, no statistically significant difference in p-STAT3 staining was observed between the progressive and static dysplasia (Fig. 6C3). These results suggest that the nucleolar expression pattern of NS may be indicative of the risk of low-grade dysplasia in progression to OSCCs. To predict the risk of low-grade OPLs in developing OSCCs, we propose a risk-assessment model based on the number of cells with nucleolar NS signals per 10,000 μm^2 in the lower half or the whole epithelial thickness, based on our current findings (Fig. 6D1). In this model, OPL samples with 25 or more NS^+ cells/10,000 μm^2 are predicted to develop OSCCs in five years, whereas those with less than 25 NS^+ cells/10,000 μm^2 are predicted to remain static, with a p-value of 0.029 as calculated by the Chi-square test (Fig. 6D2).

Discussion

Patients diagnosed with OSCC have relatively low survival rates and often live with severe complications caused by the treatment. Finding reliable biomarkers to either detect early neoplastic lesions or predict the risk of low-grade dysplasia in becoming cancer is critical for making correct decisions on treatment plan, especially for patients with large, diffuse, multifocal, and/or recurrent lesions. In this study, we investigated the expression profiles of NS and p-STAT3 in oral precancerous and cancerous lesions using a 4NQO-induced oral carcinogenesis rat model, archival human biopsy samples of epithelial dysplasia and OSCC, and low-grade dysplasia samples with long-term follow-up information.

NS and p-STAT3 expression for early cancer detection

Oral carcinogenesis is a multi-step process driven by early transforming events in OPLs that lead to uncontrolled cell proliferation and invasion in OSCCs. Gene products involved in the early events driving the transformation of OPLs to OSCCs are reasonable candidates for predicting the risk of OPLs in becoming OSCCs. Expression patterns of many stem cell factors in cancers have also been implicated as predictive, diagnostic, and/or prognostic markers. For diagnostic (stage-specific) markers, expression changes may occur in: (1) both dysplastic and OSCC lesions compared to normal tissue, (2) OSCCs but not normal or dysplastic tissues, or (3) dysplastic and OSCC lesions with incremental changes. In this study, we examined NS and one of its downstream targets, p-STAT3, to determine their potential application in detecting dysplasia and OSCCs or predicting the progression risk of OPLs. Our results showed that the NS and p-STAT3 signal intensity were most significantly increased during the transition from normal to hyperplasia in rat samples. In human samples, their signals were elevated in high-grade dysplasia and poorly differentiated OSCC compared to low-grade dysplasia and well differentiated OSCC, respecitvely. The distribution and number of NS and p-STAT3-positive cells increased as lesions advanced from hyperplastic to low-grade and high-grade dysplastic lesions. Our p-STAT3 findings are consistent with previous studies showing that nuclear p-STAT3 was elevated in oral leukoplakia (with or without dysplasia) and OSCC [25]. Together, these findings indicate that the positive cell number and distribution of NS and p-STAT3 may be used to assist in diagnosing early precancerous lesions. Of note, our results showed that NS and p-STAT3 display overlapping but non-identical patterns of expression, indicating that additional regulatory components may be involved in either the nucleostemin or the STAT3 signaling pathway.

Genetic markers can also be used in cancer detection, diagnosis and prognosis. Wide-spread genetic mutations, amplifications (GOH), and

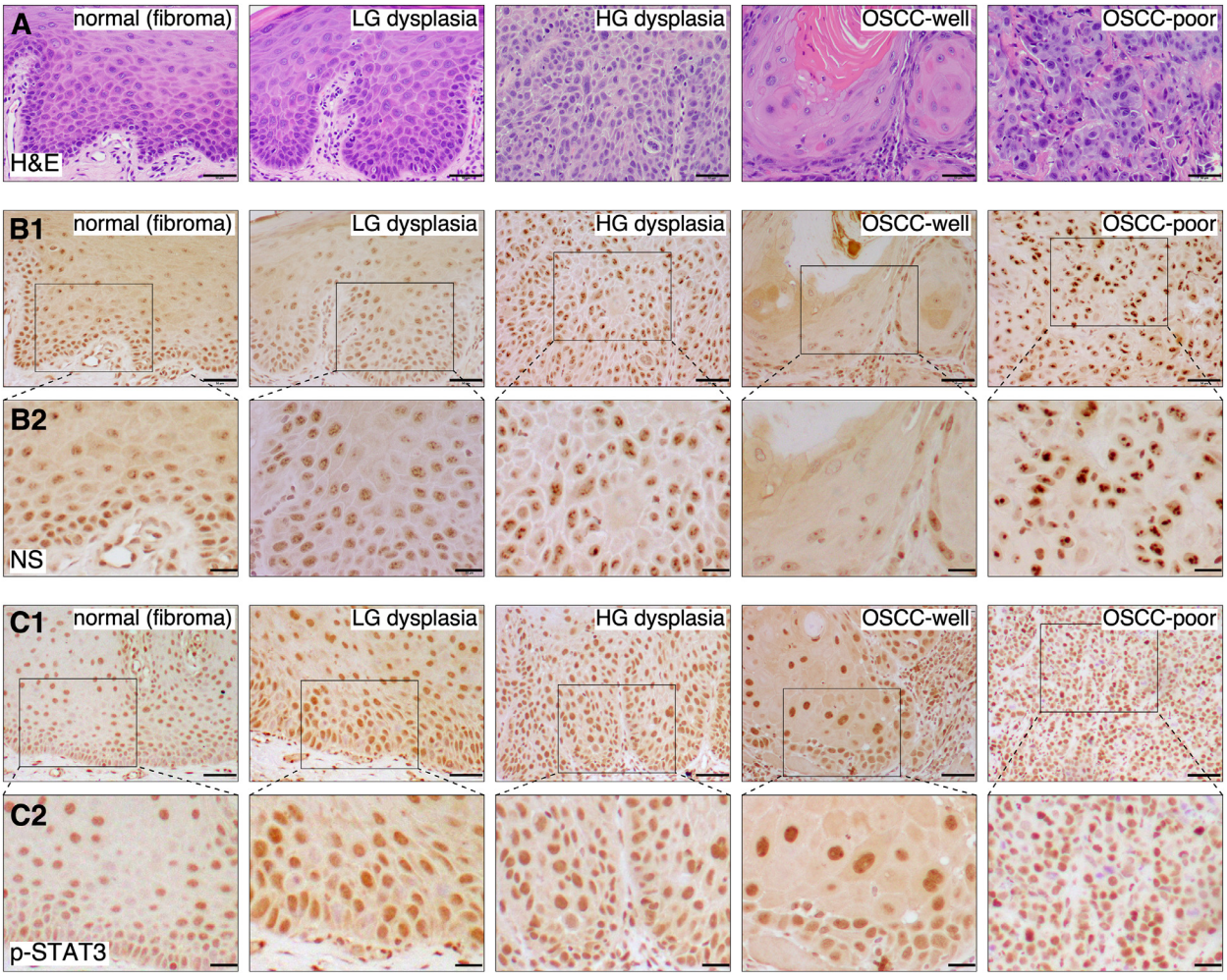

Fig. 4. Expression of NS and p-STAT3 in human archival samples of epithelial dysplasia and OSCC lesions. (A) H&E of normal oral squamous epithelium (fibroma), low-grade dysplasia, high-grade dysplasia, well differentiated (OSCC-well) and poorly differentiated SCC (OSCC-poor). Immunohistochemistry of NS (B) and p-STAT3 (C) on adjacent sections. All IHC images were counterstained with hematoxylin (blue/purple) on top of DAB signals (brown). Scale bars show 50 μm for (A, B1, C1) and 20 μm for (B2, C2).

deletions (LOH) have been shown in connection with the development of oral preneoplastic/neoplastic lesions. Genetic markers are more representative of cellular changes that occur permanently compared to IHC markers. While genetic markers may be more indicative of lesion eradication [32], they are not readily applicable to detecting changes at the cellular level. Many genetic mutations and chromosome abnormalities accumulate as a result of bystander events during the process of tumor evolution, which is consistent with our findings that quantitative changes in genetic markers were observed most commonly in neoplastic lesions. In addition, it remains a challenge to determine genetic alterations in focal lesions within the epithelium.

NS and p-STAT3 expression for predicting cancer risk in precancerous lesions

In human dysplasia samples with longitudinal clinical data, the number of cells with NS nucleolar signals is significantly higher in progressive dysplasia than in static dysplasia. These results suggest that the NS nucleolar signal may be useful for predicting the risk of dysplasia in developing OSCC (Fig. 6E). The potential use of NS as a risk-predictive marker for dysplasia is clinically appealing, as it would allow for the distinction between high-risk vs. low-risk dysplasia and employing more definitive treatment of high-risk dysplasia without introducing unnecessary complications to patients with low-risk dysplasia. To date, the literature on cancer-predictive markers found in dysplasia is extremely limited. Instead, most published studies are centered on markers that differentiate dysplasia and OSCC, which are useful for disease diagnosis and early detection but not for predicting cancer risk or survival outcome. Our longitudinal study provides a novel glimpse into this question that may also shed light on the underlying mechanism driving the progression of dysplasia to OSCC. However, the use of immunohistochemistry in identifying biomarkers for the risk of dysplasia to OSCC conversion is not without issues caused by, for the most part, technical variability (*e.g.*, tissue processing and IHC procedures) and individual variability (*e.g.*, disease and clinicodemographic heterogeneity). Furthermore, the interpretation of positive signals may also be challenging. We observed a nucleolar pattern of NS signals that is more abundant in progressive dysplasia ($p = 0.05$) and a diffuse nuclear pattern of NS signals more abundant in static dysplasia ($p = 0.10$). Given that NS is a nucleolar protein, questions arise regarding the validity of the diffuse nuclear signal. A previous study has reported a similar finding, *i.e.*, a nucleolar and a nuclear NS staining pattern, in undifferentiated proliferative cells, such as human germ cell tumors and mouse teratoma models [33]. Therefore, a prominent NS signal in the nucleolus may indicate hyperactive nucleolar activity in ribosomal biosynthesis or other non-ribosome-related cell biological functions [34], whereas cells with a diffuse nuclear NS signal may experience a low nucleolar activity and not be as

A

	Code	Location	1st Biopsy	2nd Biopsy	Interval
Progressive	P1	ventral tongue	Moderate dysplasia	squamous cell carcinoma	3 yr
	P2	left tongue	Mild dysplasia	squamous cell carcinoma	2 yr
	P3	right tongue	Mild dysplasia	squamous cell carcinoma	3 yr
	P4	right tongue	Mild dysplasia	squamous cell carcinoma	2 yr
Static	S1	right tongue	Mild dysplasia	Mild dysplasia	14 yr
	S2	ventral tongue	Mild dysplasia	Mild dysplasia	7 yr
	S3	left tongue	Moderate dysplasia	Moderate dysplasia	10 yr
	S4	left tongue	Moderate dysplasia	Mild dysplasia	9 yr

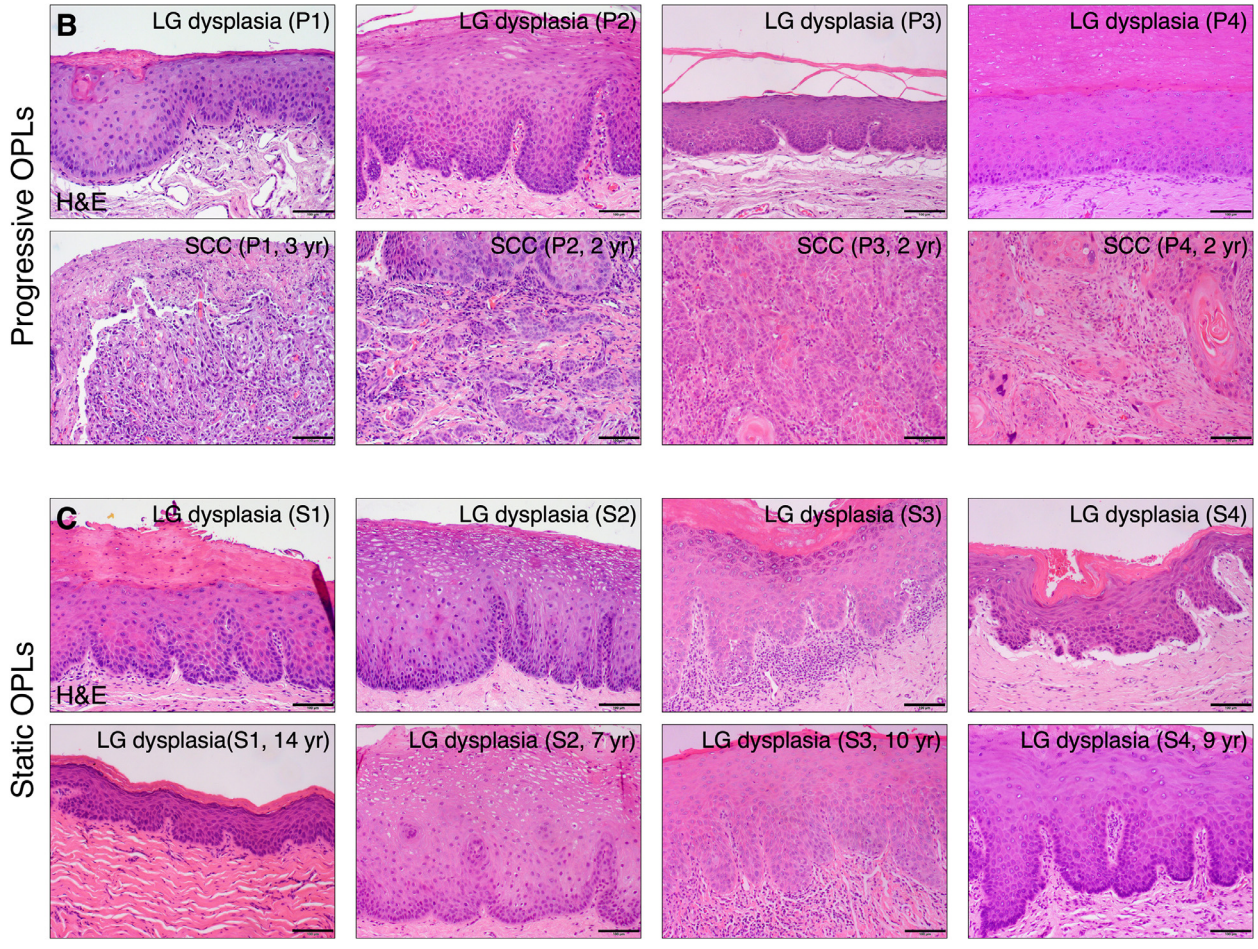

Fig. 5. Human dysplasia/OSCC samples with multiple biopsies and longitudinal clinical follow-up information (A) Eight patients with low-grade dysplastic lesions in their first biopsy but different progression outcomes. Lesions in the progressive group became OSCC in 2 or 3 years, whereas lesions in the static group remained low-grade for 7–14 years. H&E staining of 1st biopsy samples (top) and follow-up biopsy samples (bottom) in the progressive group (B) or the static group (C). Scale bars show 100 μm.

proliferative as their nucleolar counterparts. So far, our study has not yet established a statistically significant difference in the NS nuclear or p-STAT3 signal between the progressive and static dysplasia, which may be due to the small sample size, as the collection of longitudinal samples, especially those in the static group, is limited by time. Notably, p-STAT3 was shown to be up-regulated not only in the tumor epithelium but also in the tumor-surrounding normal epithelium of HNSCC patients [35].

Preclinical models of oral carcinogenesis for biomarker discovery and validation

To date, few cancer markers have been successfully validated for clinical application. The challenges include the length of time required to conduct prospective human studies, the number of samples needed for robust power analysis, and the heterogeneity of human populations. Preclinical

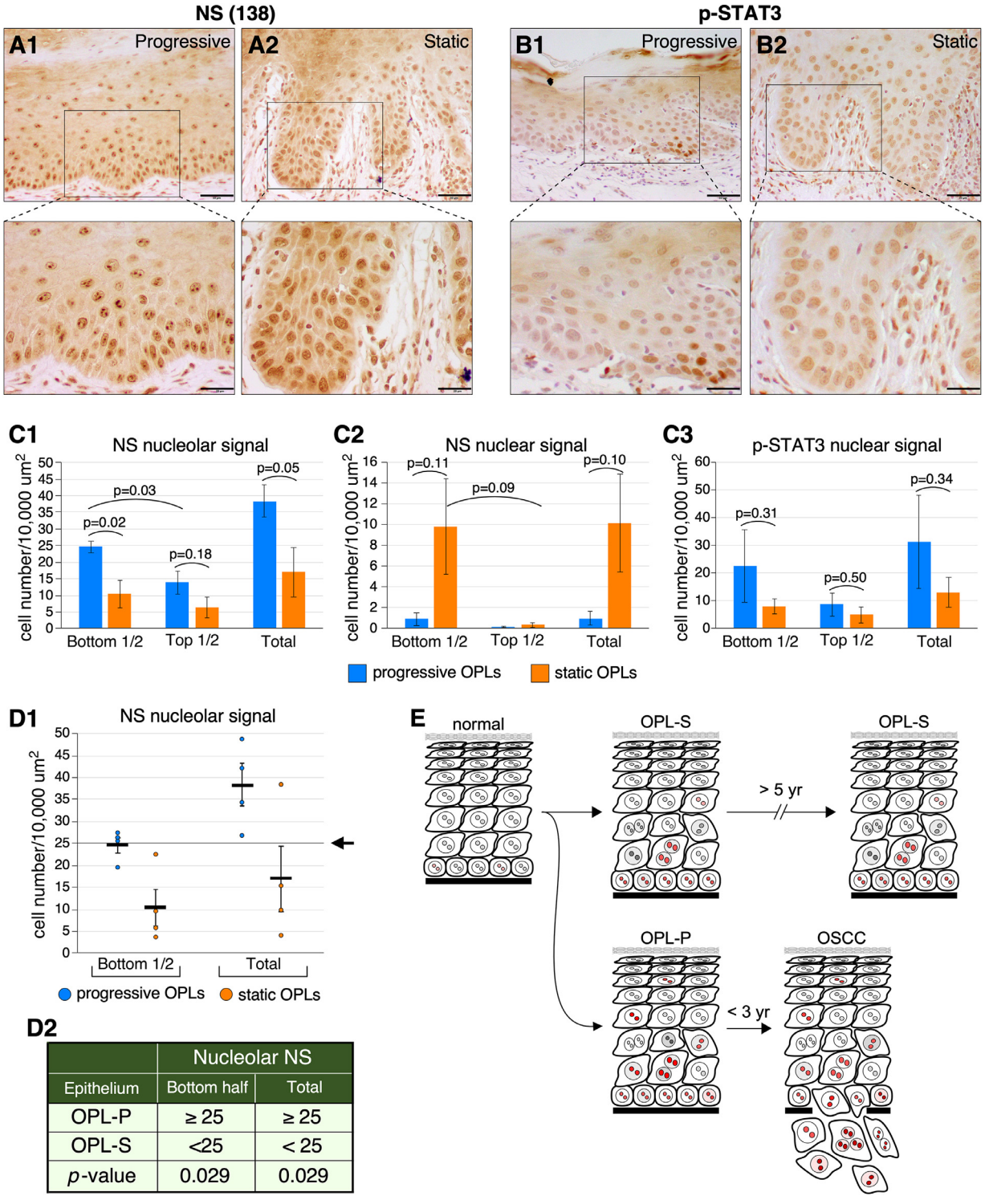

	Nucleolar NS	
Epithelium	Bottom half	Total
OPL-P	≥ 25	≥ 25
OPL-S	<25	< 25
p-value	0.029	0.029

Fig. 6. Expression profiles of NS and p-STAT3 in the progressive vs. static human dysplasia samples (A) NS signals in the progressive (A1) vs. static (A2) low-grade dysplastic lesions. (B) p-STAT3 signals in the progressive (B1) vs. static (B2) low-grade dysplastic lesions. All IHC images were counterstained with hematoxylin (blue/purple) on top of DAB signals (brown). (C) Comparison between progressive vs. static OPLs on their NS (C1, C2) and p-STAT3 (C3) expression profiles (intensity and distribution) was quantified using a nonparametric two-tailed TTEST. Scale bars show 50 μm. Bar graphs show means (± s.e.m). (D1) Numbers of cells with nucleolar NS signals per 10,000 μm^2 in the bottom half or the whole epithelial thickness in individual cases of progressive (OPL-P, blue circles) and static (OPL-S, orange circles) low-grade oral dysplasia. The arrow points to the proposed cut-off at 25 cells/10,000 μm^2. (D2) A proposed risk-assessment model based on the density of nucleolar NS+ cells (cells per 10,000 μm^2) to predict the progressive vs. static outcome of low-grade oral dysplasia. *P*-values were calculated by the chi-square test. (E) Diagram depicting the different patterns of cells with nucleolar NS signals, indicated in red, in OPL-P vs. OPL-S. (For interpretation of the references to color in this figure legend, the reader is referred to the web version of this article).

models may provide alternatives for marker discovery or validation. Several animal models have been used to study oral carcinogenesis [28,31,36–40]. The 7,12-dimethylbenzanthracene-induced hamster cheek pouch model, although common, has different histologic, anatomical, and genetic features from human OSCC. In contrast, the 4NQO rodent model exhibits several features characteristic of human OPLs and OSCCs, including lesion location, histology, gene expression profile, and formation of DNA adducts, which play a central role in the pathogenesis of tobacco-associated carcinogenesis [28,36,41–43]. Due to the limitation of animal health consideration, only well differentiated but not poorly differentiated OSCCs were observed in our 4NQO model. One concern in using preclinical models is how close in resemblance they are in mimicking human diseases. Human OSCC is a complex disease with multiple risk factors, including tobacco, alcohol, human papilloma virus (HPV), and diet. Tobacco is the most common risk factor for OSCC. Alcohol is an independent risk factor for OSCC among non-smokers, but can enhance the carcinogenic effect of tobacco. HPV (E2, E6, and E7) has been established as a distinct clinical entity with a better treatment outcome [44]. Therefore, biomarkers for predicting the outcome of OSCC of different etiologies may conceivably be different. Finally, one technical limitation in working with preclinical animals is the size of their lesions, which makes repetitive biopsy of the same lesion sites extremely challenging, if not impossible.

In conclusion, this study reveals NS expression and STAT3 activation as early events in human and rodent oral dysplastic and OSCC lesions and raises a potential use of NS and p-STAT3 for early detection of OSCC and cancer risk assessment of OPL.

Declaration of Competing Interest

The authors declare no conflict of interest.

CRediT authorship contribution statement

Madeleine Crawford: Data curation, Formal analysis, Writing – review & editing. **Xiaoqin Liu:** Data curation, Formal analysis. **Yi-Shing L Cheng:** Conceptualization, Data curation, Formal analysis, Writing – review & editing. **Robert YL Tsai:** Conceptualization, Data curation, Formal analysis, Funding acquisition, Supervision, Writing – original draft, Writing – review & editing.

Acknowledgments

We thank Eliza Johnson for her help in analyzing the image areas and Dr. Stefan Siwko for reviewing the manuscript before submission. This work was supported by Cancer Prevention and Research Institute of Texas (CPRIT) Early Translational Research Award (RP170179) to Robert YL Tsai and Yi-Shing L Cheng.

Supplementary materials

Supplementary data associated with this article can be found, in the online version, at doi:10.1016/j.neo.2021.11.001.

References

[1] Neville BW, et al. Squamous cell carcinoma. In: *Oral and Maxillofacial Pathology*. St. Louis: Saunders Elsevier; 2016. p. 409–21.

[2] Chi AC. Leukoplakia (Leukokeratosis; erythroleukoplakia). In: BW Neville, editor. *Oral and Maxillofacial Pathology*. St. Louis: Saunders Elsevier; 2016. p. 388–97. et al., Editors.

[3] Rivera C, et al. Prognostic biomarkers in oral squamous cell carcinoma: a systematic review. *Oral Oncol* 2017;**72**:38–47.

[4] Liu W, et al. Expression patterns of cancer stem cell markers ALDH1 and CD133 correlate with a high risk of malignant transformation of oral leukoplakia. *Int J Cancer* 2013;**132**(4):868–74.

[5] Tsai RY. Balancing self-renewal against genome preservation in stem cells: how do they manage to have the cake and eat it too? *Cell Mol Life Sci* 2016;**73**(9):1803–23.

[6] Tsai RY, McKay RD. A nucleolar mechanism controlling cell proliferation in stem cells and cancer cells. *Genes Dev* 2002;**16**(23):2991–3003.

[7] Meng L, et al. Nucleostemin deletion reveals an essential mechanism that maintains the genomic stability of stem and progenitor cells. *Proc Natl Acad Sci U S A* 2013;**110**(28):11415–20.

[8] Tsai RY. Turning a new page on nucleostemin and self-renewal. *J Cell Sci* 2014;**127**(18):3885–91.

[9] Tsai RY. New frontiers in nucleolar research: nucleostemin and related proteins. *Nucleolus Protein Rev* 2011;**15**:301–20.

[10] Lin T, et al. A novel role of nucleostemin in maintaining the genome integrity of dividing hepatocytes during mouse liver development and regeneration. *Hepatology* 2013;**58**(6):2176–87.

[11] Yasumoto H, et al. GNL3L inhibits activity of estrogen-related receptor-gamma by competing for coactivator binding. *J Cell Sci* 2007;**120**(15):2532–43.

[12] Meng L, Hsu JK, Tsai RY. GNL3L depletion destabilizes MDM2 and induces p53-dependent G2/M arrest. *Oncogene,* 2011;**30**(14):1716–26.

[13] Lin T, et al. Nucleostemin and GNL3L exercise distinct functions in genome protection and ribosome synthesis, respectively. *J Cell Sci* 2014;**127**(10):2302–12.

[14] Lin T, et al. Tumor-initiating function of nucleostemin-enriched mammary tumor cells. *Cancer Res* 2010;**70**(22):9444–52.

[15] Hua L, et al. Upregulated expression of Nucleostemin/GNL3 is associated with poor prognosis and sorafenib resistance in hepatocellular carcinoma. *Pathol Res Pract* 2017;**213**(6):688–97.

[16] Lin T, et al. Nucleostemin reveals a dichotomous nature of genome maintenance in mammary tumor progression. *Oncogene* 2019;**38**(20):3919–31.

[17] Wang J, et al. Nucleostemin modulates outcomes of hepatocellular carcinoma via a tumor adaptive mechanism to genomic stress. *Mol Cancer Res* 2020;**18**(5):723–34.

[18] Cada Z, et al. Nucleostemin expression in squamous cell carcinoma of the head and neck. *Anticancer Res* 2007;**27**(5A):3279–84.

[19] Yoshida R, et al. Nucleostemin affects the proliferation but not differentiation of oral squamous cell carcinoma cells. *Cancer Sci* 2011;**102**(7):1418–23.

[20] Yoshida R, et al. Overexpression of nucleostemin contributes to an advanced malignant phenotype and a poor prognosis in oral squamous cell carcinoma. *Br J Cancer* 2014;**111**(12):2308–15.

[21] Okamoto N, et al. Maintenance of tumor initiating cells of defined genetic composition by nucleostemin. *Proc Natl Acad Sci U S A* 2011;**108**(51):20388–93.

[22] Zhang X, et al. Nucleostemin promotes hepatocellular carcinoma by regulating the function of STAT3. *Exp Cell Res* 2020;**387**(1):111748.

[23] Zhong Z, Wen Z, Darnell JE. Stat3: a STAT family member activated by tyrosine phosphorylation in response to epidermal growth factor and interleukin-6. *Science* 1994;**264**(5155):95–8.

[24] Shah NG, et al. Stat3 expression in oral squamous cell carcinoma: association with clinicopathological parameters and survival. *Int J Biol Mark* 2006;**21**(3):175–83.

[25] Macha MA, et al. Prognostic significance of nuclear pSTAT3 in oral cancer. *Head Neck* 2011;**33**(4):482–9.

[26] Vitale-Cross L, et al. Chemical carcinogenesis models for evaluating molecular-targeted prevention and treatment of oral cancer. *Cancer Prev Res* 2009;**2**(5):419–22 (Phila).

[27] Hasina R, et al. ABT-510 is an effective chemopreventive agent in the mouse 4-nitroquinoline 1-oxide model of oral carcinogenesis. *Cancer Prev Res* 2009;**2**(4):385–93 (Phila).

[28] Tang XH, et al. Oral cavity and esophageal carcinogenesis modeled in carcinogen-treated mice. *Clin Cancer Res* 2004;**10**(1):301–13 Pt 1.

[29] Kanojia D, Vaidya MM. 4-nitroquinoline-1-oxide induced experimental oral carcinogenesis. *Oral Oncol* 2006;**42**(7):655–67.

[30] Meng L, Lin T, Tsai RY. Nucleoplasmic mobilization of nucleostemin stabilizes MDM2 and promotes G2-M progression and cell survival. *J Cell Sci* 2008;**121**(Pt 24):4037–46.

[31] Tanuma J, et al. Genetic predisposition to 4NQO-induced tongue carcinogenesis in the rat. *Med Princ Pract* 2005;**14**(5):297–305.

[32] Mao L, et al. Phenotype and genotype of advanced premalignant head and neck lesions after chemopreventive therapy. *J Natl Cancer Inst* 1998;**90**(20):1545–51.

[33] Uema N, et al. Abundant nucleostemin expression supports the undifferentiated properties of germ cell tumors. *Am J Pathol* 2013;**183**(2):592–603.

[34] Pederson T, Tsai RY. In search of non-ribosomal nucleolar protein function and regulation. *J Cell Biol* 2009;**184**(6):771–6.

[35] Grandis JR, et al. Constitutive activation of Stat3 signaling abrogates apoptosis in squamous cell carcinogenesis *in vivo*. *Proc Natl Acad Sci U S A* 2000;**97**(8):4227–32.

[36] Nauta JM, et al. Comparison of epithelial dysplasia–the 4NQO rat palate model and human oral mucosa. *Int J Oral Maxillofac Surg* 1995;**24**(1):53–8 Pt 1.

[37] Nauta JM, et al. Epithelial dysplasia and squamous cell carcinoma of the Wistar rat palatal mucosa: 4NQO model. *Head Neck* 1996;**18**(5):441–9.

[38] Kitano M. Host genes controlling the susceptibility and resistance to squamous cell carcinoma of the tongue in a rat model. *Pathol Int* 2000;**50**(5):353–62.

[39] Hawkins BL, et al. 4NQO carcinogenesis: a mouse model of oral cavity squamous cell carcinoma. *Head Neck* 1994;**16**(5):424–32.

[40] Gimenez-Conti IB, Slaga TJ. The hamster cheek pouch model of carcinogenesis and chemoprevention. *Adv Exp Med Biol* 1992;**320**:63–7.

[41] Nishimura A. Changes in Bcl-2 and Bax expression in rat tongue during 4-nitroquinoline 1-oxide-induced carcinogenesis. *J Dent Res* 1999;**78**(6):1264–9.

[42] Sato K, et al. Expression of beta-catenin in rat oral epithelial dysplasia induced by 4-nitroquinoline 1-oxide. *Oral Oncol* 2002;**38**(8):772–8.

[43] Hecht SS. Cigarette smoking and lung cancer: chemical mechanisms and approaches to prevention. *Lancet Oncol* 2002;**3**(8):461–9.

[44] Dok R, Nuyts S. HPV positive head and neck cancers: molecular pathogenesis and evolving treatment strategies. *Cancers* 2016;**8**(4):41 (Basel).